

FIG. 1. Low energy neutrons from the disintegration of  $\text{Li}^7$  by deuterons. The curve on which the probable errors have been indicated has been corrected for variation with energy of  $n-p$  scattering cross section and acceptance probability.

A 100-kev thick target of  $\text{Li}_2\text{SO}_4$ , in which the Li was 99.8 percent  $\text{Li}^7$ , was bombarded with 1.1-Mev deuterons from the Bartol Van de Graaff generator, and Ilford  $\text{C}_2$  plates 10 cm from the target at  $0^\circ$  to the beam were irradiated with the reaction neutrons for approximately  $5 \mu\text{hr}$ . The recoil protons with ranges less than  $210 \mu$  and an acceptance angle of  $15^\circ$  were counted. The angle between the direction of the beam and the recoil proton in the horizontal plane of the plate were recorded and the energies corrected according to the relation  $E^2 = E_n^2 \cos^2 \theta$ . Seven hundred tracks were measured and these are plotted in 0.2-Mev intervals in Fig. 1.

Besides the continuum of neutrons from  $\text{Li}^7 + d \rightarrow \text{He}^4 + \text{He}^3$ ,  $\text{He}^3 \rightarrow \text{He}^4 + n$  there are two groups of neutrons which must arise from the reaction  $\text{Li}^7 + d \rightarrow \text{Be}^8 + n$ , at 1.36 and 4.9 Mev and give levels in  $\text{Be}^8$  at 14.7 and 11.1 Mev; neutrons from carbon would give a group at approximately 0.8 Mev. The general shape of the curve agrees with that of Staub and Stevens, both curves having a peak at approximately 1.5 and 5 Mev besides the continuum.

\* Assisted by the joint program of the ONR and AEC.

<sup>1</sup> H. Staub and W. E. Stephens, Phys. Rev. **55**, 845 (1939).

<sup>2</sup> H. T. Richards, Phys. Rev. **59**, 796 (1941).

<sup>3</sup> L. L. Green and W. M. Gibson, Proc. Phys. Soc. London **62**, 407 (1949).

<sup>4</sup> Furnished by Y-12 Plant, Oak Ridge, Tennessee.

## A Measurement of the Positive $\pi$ - $\mu$ -Decay Lifetime\*

O. CHAMBERLAIN, R. F. MOZLEY, J. STEINBERGER, AND C. WIEGAND  
Radiation Laboratory, Department of Physics, University of California,  
Berkeley, California  
June 5, 1950

THE lifetime of  $\pi$ -mesons was first measured by Richardson<sup>1</sup> and later by Martinelli and Panofsky.<sup>2</sup> The method was the same in both cases: the fraction of  $\pi$ -mesons surviving various

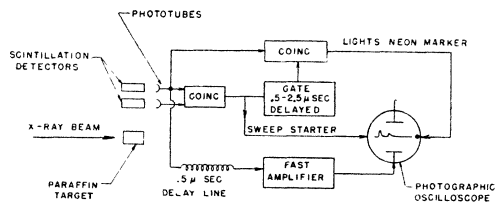


FIG. 1. Block diagram of apparatus.

times of flight was measured by placing photographic detectors at various path lengths from a target in which  $\pi$ -mesons were produced.

In the experiment reported here we have observed the decay of  $\pi$ -mesons through the light emitted by a *trans*-stilbene crystal in which the decay events occur. The mesons were produced in a paraffin target which was placed in the x-ray beam of the 340-Mev synchrotron. The mesons of interest here passed through the first crystal and came to rest in the second crystal. There were three bursts of light from the second crystal when (1) the meson came to rest, (2) the (positive)  $\pi$ -meson decayed to a  $\mu$ -meson which also came to rest in the crystal, and (3) the  $\mu$ -meson decayed to a positron which escaped from the crystal. Photo-multiplier tubes were used to detect the light from the stilbene crystals.

As outlined in Fig. 1, a coincidence between the two detectors was used to start the sweep ( $10^{-8}$  sec./mm) of an oscilloscope and to initiate a delayed gate circuit (gate open from 0.5 to 2.5  $\mu\text{sec}$ ). The output of the second detector was delayed  $0.5 \times 10^{-6}$  sec., amplified in a fast distributed amplifier, and fed to the vertical deflection plates of the oscilloscope. The oscilloscope traces, which were recorded photographically on a continuously moving film,

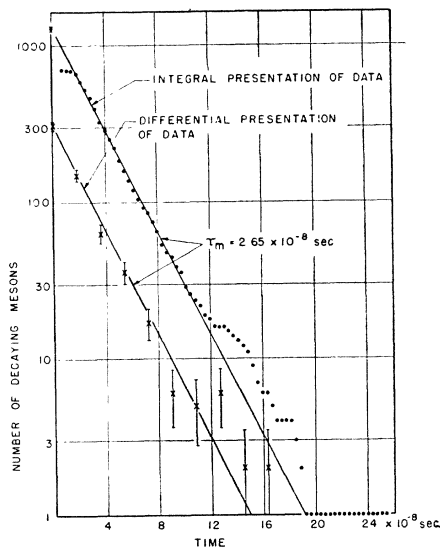


FIG. 2. Decay rate of the positive  $\pi$ -meson. The zero-time point on the integral curve represents all marked traces minus accidental traces. The zero-time point on the differential curve represents those traces with pulse separation between  $2.17$  and  $3.98 \times 10^{-8}$  sec., the next point those between  $3.98$  and  $5.79 \times 10^{-8}$  sec., etc.

showed in every case the pulse which initiated the sweep. If the responsible particle was a  $\pi^+$ -meson which stopped in the crystal, and if the meson lived at least  $2 \times 10^{-8}$  sec. before decaying to a  $\mu$ -meson, then two pulses were seen on the trace. Measurement of the separation of these two pulses determined the life span of that meson. On some traces a third pulse was seen due to the  $\mu$ -meson decay, although in most instances the sweep was finished before the  $\mu$ -meson decayed. The purpose of the 0.5- to 2.5- $\mu\text{sec}$ . delayed gate was to detect electronically the  $\mu$ -meson decay. When a pulse fell within this gate time a neon bulb at the edge of the oscilloscope face flashed.

We consider only those pulses marked by a neon bulb flash. By so doing, we use a group of pulses constituted as follows. Five percent are background due to accidental coincidences of extraneous pulses with the delayed gate; three percent are  $\mu$ -mesons formed by  $\pi$ -mesons which decayed in flight; 92 percent (1302 in number) are  $\pi^+$ -mesons stopped in the crystal. A total of 554 traces showed two distinct pulses whose separations could be measured with certainty.

In the differential interpretation of these data we ignore part of the information and consider only those 554 mesons which lived longer than  $2.18 \times 10^{-8}$  sec., so the time of their decay is accurately known. The information used is that shown in the differential decay curve of Fig. 2, where the curve is displaced toward the left to separate the two curves. The alternative integral interpretation takes account of the fact that the number of mesons decaying before  $2.18 \times 10^{-8}$  sec. (748) is also known, and so their mean life can be estimated. The integral decay curve of Fig. 2 shows the number of mesons decaying after time  $t$  vs.  $t$ .

The greater statistical accuracy obtainable with the integral interpretation is offset by the limited accuracy with which the total number of mesons stopped can be determined.

The mean life (with the calculated standard deviation) is:

$$\begin{aligned} \tau &= (2.65 \pm 0.12) \times 10^{-8} \text{ sec. (differential interpretation),} \\ \tau &= (2.59 \pm 0.12) \times 10^{-8} \text{ sec. (integral interpretation).} \end{aligned}$$

The previously reported values are

$$\begin{aligned} \tau &= \left(1.11 \pm \frac{0.45}{0.35}\right) \times 10^{-8} \text{ sec. (Richardson),} \\ \tau &= \left(1.97 \pm \frac{0.21}{0.25}\right) \times 10^{-8} \text{ sec. (Martinelli and Panofsky).} \end{aligned}$$

While this note was in preparation a third measurement has been reported by Kraushaar, Thomas, and Henri.<sup>3</sup> Using a method somewhat similar to ours they find that

$$\tau = (1.65 \pm 0.33) \times 10^{-8} \text{ sec.}$$

We wish to thank Professors E. McMillan and E. Segrè for their encouragement.

\* This work was supported by the AEC.

<sup>1</sup> J. Richardson, Phys. Rev. **74**, 1720 (1948).

<sup>2</sup> E. A. Martinelli and W. K. H. Panofsky, Phys. Rev. **77**, 465 (1950).

<sup>3</sup> Kraushaar, Thomas, and Henri, Phys. Rev. **78**, 486 (1950).

## The Coherent Neutron Scattering Cross Sections of Nickel and Its Isotopes

W. C. KOEHLER, E. O. WOLLAN, AND C. G. SHULL  
Oak Ridge National Laboratory, Oak Ridge, Tennessee  
May 26, 1950

THE coherent scattering cross section of normal nickel has been found from neutron diffraction measurements to be 13.5 barns.<sup>1</sup> The total scattering cross section has been measured by the Columbia group to be 17.0 barns.<sup>2</sup> Since the three major isotopic constituents of nickel are even-even isotopes, it is reasonable to ascribe the difference between the total and coherent

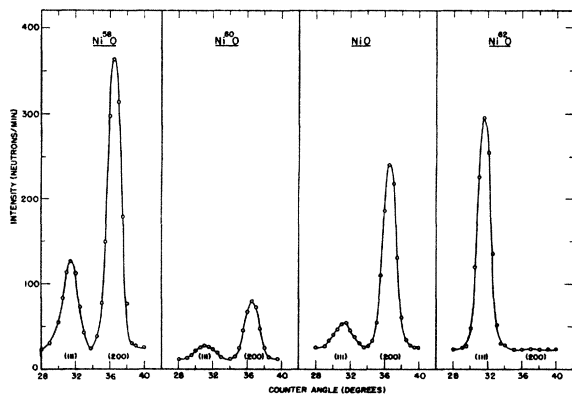


FIG. 1. Partial neutron diffraction patterns of isotopically enriched samples of NiO.

TABLE I. Scattering amplitudes and cross sections.

Isotope	Coherent scattering amplitude ( $10^{-12}$ cm)	$\sigma$ (barns)	Contribution to normal nickel amplitude ( $10^{-12}$ cm)
Ni <sup>58</sup>	1.48	27.6	1.00
Ni <sup>60</sup>	0.28	0.97	0.073
Ni <sup>62</sup>	-0.85	9.1	-0.032
Ni	1.03	13.3	-0
			Total 1.04

scattering cross sections to the isotope effect, and since this difference is large it might be expected that the scattering properties of the different isotopes would be widely different. Accordingly, samples of nickel oxide (NiO) enriched in Ni<sup>58</sup>, Ni<sup>60</sup>, and Ni<sup>62</sup> were studied with the crystal spectrometer. The scattering cross sections of Ni<sup>58</sup> and Ni<sup>60</sup> had been previously measured in this laboratory,<sup>1</sup> but under less favorable conditions than existed for the present set of measurements.

NiO is also of interest because of its magnetic properties. The neutron diffraction patterns of the various oxides all show, in addition to the nuclear peaks which vary from isotope to isotope, antiferromagnetic reflections which are identical in all samples within experimental error. Preliminary results of the magnetic scattering experiments have been given by Shull,<sup>3</sup> and a detailed report will be made at a later date.

In Fig. 1 are shown portions of the diffraction patterns obtained from the four oxide samples studied. These have all been normalized so that a direct comparison of the peak intensities can be made. The interpretation of the diffuse scattering is complicated by the fact that it is contributed to by isotopic diffuse scattering, multiple scattering, and scattering by the sample window, so that a direct comparison of the diffuse scattering in the patterns is not permissible. Since NiO has the rocksalt structure, a simple inspection of the diffraction pattern is sufficient to establish the phase of scattering of the nickel isotopes relative to that of oxygen. Clearly all scatter with positive phase except Ni<sup>62</sup>, as evidenced by the very weak or absent (200) reflection in the pattern of Ni<sup>62</sup>O.

The effective scattering amplitudes obtained from the isotopically enriched oxides were corrected for isotopic impurity and the resultant coherent scattering amplitudes and cross sections are given in Table I. In addition, the contribution of each of the isotopes to the normal nickel amplitude has been calculated, and the sum compared with the nickel amplitude as measured directly. The agreement between these two results is excellent.

As one sees, these three isotopes of nickel show marked differences in their scattering properties. In each case the scattering cross section differs widely from the potential scattering which has a value for Ni of about 4.4 barns,<sup>4</sup> and hence there must be a strong contribution from resonance effects. In the case of Ni<sup>58</sup>, which has an unusually large cross section, a virtual resonance is indicated since only for  $E > E_r$  does one get large cross sections due to constructive interference between potential and resonance scattering. The small cross section for Ni<sup>60</sup> most probably corresponds to a point near the minimum arising from destructive interference between potential and resonance scattering, and hence to a positive energy resonance. The relatively large negative scattering amplitude found for Ni<sup>62</sup> must also correspond to a positive energy resonance. The only definitely known resonance for nickel that could account for either of these observed cross sections falls<sup>5</sup> at 3600 ev. For a resonance level at this energy to be responsible on the basis of the one level Breit-Wigner formula for either of the above observed thermal scattering amplitudes requires a neutron width of the order of 1000 ev.

<sup>1</sup> C. G. Shull and E. O. Wollan (unpublished work). Bernstein, Dial, Stanford, and Stephenson, Phys. Rev. **75**, 1302 (1949).

<sup>2</sup> Havens, Rainwater, Wu, and Dunning, Phys. Rev. **73**, 963 (1948).

<sup>3</sup> C. G. Shull, Phys. Rev. **78**, 638T (1950).

<sup>4</sup> Feshbach, Peaslee, and Weisskopf, Phys. Rev. **71**, 145 (1947).

<sup>5</sup> Ruderman, Havens, Taylor, and Rainwater, Phys. Rev. **75**, 1296 (1949).